From Land Use to Functional Spaces: Characterizing the Urbanization Dynamics of the Beijing-Tianjin-Hebei Region through Production-Living-Ecological Spaces Patterns

Bin Liu[1,2]

1. State Key Laboratory of Regional and Urban Ecology, Research Center for Eco-Environmental Sciences, Chinese Academy of Sciences, Beijing 100085, China

2. University of Chinese Academy of Sciences, Beijing 100049, China

Abstract: Regions represent complex landscapes where production, living, and ecological functions intersect, yet rapid urbanization has exacerbated conflicts within the human-land-environment system, resulting in the disordered construction of functional spaces. To address these challenges and optimize territorial spatial planning, China introduced the concept of production-living-ecological spaces (PLEs) in 2012. The evolution of PLEs strongly reflects the land-human activity interactions driven by human needs amid urbanization, yet few studies have quantitatively characterized and compared the dynamics of urbanization through the lens of PLE functional spaces. Adopting a land use-to-functional space perspective, this study examines the Beijing-Tianjin-Hebei (BTH) region, which is a key area for coordinated development since 2015. By integrating POI and land use data, 5 km grid-based PLEs mapping was conducted for 2016, 2020, and 2024. Findings show BTH's urbanization is defined by mutual conversion of built-up land and farmland, plus coexisting ecological restoration and degradation. PLEs exhibit clear spatial differentiation: high-intensity living-production overlap in Beijing-Tianjin; fragmented production space expansion in their southern peripheries; and expanded but fragmented ecological spaces in Zhangjiakou-Chengde. These changes tie closely to regional coordination policies. This study offers a novel perspective and methodology for urbanization research, providing insights for balanced functional space construction and sustainable development. It also supports BTH's 2030 integration goals aligned with China's 15th Five-Year Plan.

Key Words: urbanization characterization; functional space patterns; POI data; land use change; production-living-ecological space mapping

1 Introduction

In the Anthropocene era, the region, as a huge complex landscape integrating production, living, and ecological functions, has become a central focus of sustainable development. Due to differences between land use and resource distribution, various kinds of landscapes, such as cities, rural areas, lakes, forests etc., showing functional intersections and landscape heterogeneity. Currently, rapid urbanization is occurring across the globe. Cities play a central role in human technological progress and have been the primary locations for the accumulation of an estimated 30 trillion tons of human-made materials[1]. As of 2023, the global urban population has reached 57%, with North America (83%) far exceeding the global average, while Africa (45%) and Asia (53%) remain below this

level[2]. Industrialization drives urbanization, promoting economic development and modernization. This process of urbanization is reflected in the transition from agricultural to industrial and service-based economies[3]. As a shared global challenge, the complex interplay between urbanization and the people-land-environment system has been revealed. For instance, Ebenezer Howard's "Garden City" concept, proposed in the 19th century, imagined a harmonized and sustainable urban design that connected cities with nature. This concept not only highlights the interplay between them but also underscores the accompanying significant changes in regional functional spaces.

Specifically, People's needs and preferences are the main drives behind the complex spatial patterns of region's functional spaces during urbanization. People, as both the primary element of urban development and end-users of functional spaces, play an important role in shaping urbanization processes. According to Maslow's hierarchy of needs theory, the process of fulfilling the five levels of needs (physiological, safety, social belonging, esteem, and self-actualization)[4]deeply promotes changes in urban architectural styles, modern development trajectories, and urban hierarchy classification. Particularly, regional functional spaces have gradually transformed from being primarily oriented toward agricultural production and living functions, complemented by commercial trade, into multifunctional hubs integrating economic, medical, educational, cultural, and commercial activities. This transformation has led to the rapid rise of modern cities and growing differences between urban and rural areas. Among the above process, rapid and extensive land use has provided essential resource capacity and spatial support for regional construction driven by people's needs in urbanization. Mainly through the marketization of land, which has accelerated urban expansion and economic development, attracting rapid flows of resources and population clusters into the region. As shown in the patterns of functional spaces, the increasing demands for commercial spaces, residential housing, and industrial manufacturing have led to the saturation of core built-up land. Consequently, conflicts between the people-land-environment system and urbanization have become increasingly apparent. For instance, suburban urbanization has occurred, leading to the relocation of industrial manufacturing spaces to these areas and exacerbating the spatial separation in job-housing spaces[5, 6, 7], while damaging urban residents' well-being and migrant workers' access to social security and sense of belonging. As time passes, the environment's capacity to sustain urbanization is reaching its limits, leading to worsening conflicts and severe threats to ecological spaces. Urban diseases are a particularly clear example of this. Specifically, urbanization as a primary driver of climate change[8]. In 2021, cities accounted for approximately 75% of fossil fuel-related CO_2 emissions, encompassing both household and industrial emissions[9]. Concurrently, biodiversity and biological evolution face significant threats[10, 11]. Furthermore, urbanization directly endanger food security, with about 80% of global cropland loss linked to urban expansion, particularly in Asia and Africa[12]. In agriculture, human-induced factors such as extreme heat and drought[13,14]. Urbanization has also caused a series of urban diseases, including the heat island effect[15,16], traffic congestion, and urban flooding[17]. Compounding these issues, infrastructure inequality[18]further impacts residents' quality of living and health[19]. Facing such conflicts, urbanization must strike a balance in regional functional spaces among production development, living equality, and the safeguarding of ecological space stability to achieve sustainable development.

China, as the world's most populous country with over 1.4 billion people (as of 2023) and the second-largest economy, has undergone rapid urbanization over the past four decades since its reform and opening-up in 1978[20]. The urbanization rate has increased significantly from 17.92%

in 1978 to 66.16% by 2023. Along with China's historical background as a major agricultural nation [21], these conflicts were also evident and more severe in China. In dealing with them, in 2010, China's *National Major Function-Oriented Zone Planning* was proposed to optimize national territorial spatial structures based on the principles of "developed production, affluent living, and a well-preserved ecology". Then, in 2012, the official concept of the Production-Living-Ecological Spaces (PLEs) was introduced for the first time at the 18th National Congress of the Communist Party of China. In 2013, the Central Urbanization Work Conference reaffirmed the importance of PLEs[22]. Since then, PLEs have become an important research perspective in spatial planning, attracting significant attention from scholars and urban planners. However, existing research on PLEs remains relatively limited, lacking direct research into the relationship between urbanization dynamics and PLEs. Current studies primarily rely on data sources such as land-use data, statistical data, and remote sensing data, focusing mainly on: identification and spatiotemporal distribution characteristics of PLEs[23-26]; PLEs functions[27-31]; PLEs evaluation or functional assessment, particularly coupling measurement evaluation[32-33]; and scenario simulation and prediction of PLEs[34-36].

The Beijing-Tianjin-Hebei (BTH) region, one of China's three major development regions, has experienced rapid urbanization, leading to severe "urban diseases" in Beijing and long-standing challenges related to internal development imbalances. In response, the Chinese government implemented the BTH Coordinated Development Strategy in 2015, with the primary objective of relocating Beijing's non-capital functions to restructure its functional spaces. This involves the transfer of four categories of functional spaces—general manufacturing, certain tertiary industries, social public services, and administrative institutions—out of the capital area, primarily to Tianjin and Hebei. By 2024, this strategy has led to significant changes in production, people's living standards, and the environment over the past decade. First, more than 3,000 manufacturing enterprises have moved out of Beijing, the permanent population in Beijing's six core districts has decreased by 15%, and over 9,200 hectares of vacated land have been converted into green spaces. Additionally, the construction of Beijing's sub-center and Xiong'an—key areas for relocating non-capital functions—has progressed significantly. The living environment in the sub-center has improved, and administrative as well as public institutions are gradually relocating to the area. Meanwhile, Xiong'an has developed its production and living spaces through comprehensive job-housing integration, advanced transportation networks, expanded educational facilities, and improved healthcare services[37-38]. In terms of economic structure, the share of the tertiary sector in the BTH region has increased by 9.6 percentage points to 67.7%. Regarding eco-environmental quality, PM2.5 concentrations have dropped by over 60% in 2023[37], and the water quality of Baiyangdian Lake has improved to Class III standards. Additionally, Zhangjiakou City has strengthened its role as an ecological barrier for the region, with forest coverage in the Three-North Shelterbelt Project area rising to 35.56%[37]. Although by 2024, the BTH's GDP has exceeded the five-trillion-yuan threshold over the past decade, it still lags behind the Yangtze River Delta, a world-class urban agglomeration[37]. All in all, efforts to establish an integrated regional framework by 2030 and build a world-class city agglomeration centered on the capital are still underway.

Points of Interest (POI) data, as a popular form of geospatial big data[39], along with mobile signaling and trajectory data, has gained wide application across various research areas[40-42]. POI data effectively represents socio-economic activities spatially, with significant strengths in timeliness, precision, cost-effectiveness, and attribute richness[43-45]. This unique combination of

features enables POI data to effectively address the limitations of traditional statistical data, which often lack spatiotemporal characteristics, and geospatial approaches like nighttime light data and remote sensing, which typically lack socio-economic attributes[46]. Consequently, researchers frequently employ POI data as a supplementary data source in urban geography, economic studies, and planning research[47], with applications ranging from functional space identification[48] and commercial district pattern analysis[49-50]to job-housing space recognition[51], building usage identification[42], urban built-up area extraction[52], spatial structure studies[47], [53], land use function identification[40], industrial spatial distribution analysis[41], [44], [54-56], fine-scale population mapping[45], and regional development assessment[39]. In recent years, a growing number of scholars have also utilized POI data to conduct research related to PLEs[26], [29], [57].

Thus, we select the BTH region as the research area and adopt PLEs as our research object, given the deep relationship between urbanization and functional space patterns, as well as the lack of direct research on the relationship between urbanization dynamics and PLEs. In this study, we explore urbanization from the perspective of visualizing it through the identification and mapping of PLEs. Specifically, we innovatively build an optimized mapping methodology for PLEs by integrating POI data with land use data and standardizing data classification based on the China's *Industrial classification for national economic activities* (GB/T 4757-2017). This approach not only integrates socioeconomic processes with natural ecological foundations to enhance accuracy and conciseness but also considers the heterogeneity of urban landscapes. Building on this, the study conducts a full-scale mapping of PLEs at a grid level across the BTH region, combined with land use changes, aiming to address two key scientific questions: (1) How can spatial mapping analysis quantify the interaction between urbanization and functional spaces, as well as their dynamic changes? (2) What are the spatiotemporal evolution patterns of PLEs during the implementation period of the BTH Coordinated Development Strategy (2016–2024)? Above all, this study not only provides new perspectives and methodologies for urbanization research but also offers important quantitative insights to support the final phase of the BTH region's integration goals during China's upcoming 15th Five-Year Plan period.

The following structure of this research is presented in four parts. Firstly, Section 2 describes the study area, the research data employed, and the methodology of the study. Secondly, Section 3 presents the results, including land use changes, the mapping and spatiotemporal patterns of PLEs in 2016, 2020, and 2024, and the urbanization dynamics characterized by land use changes and PLEs patterns. Then, Section 4 discusses the evaluation of the BTH Coordinated Development Strategy through PLEs, the advantages of the methodology, and its limitations. Finally, Section 5 provides the conclusions, the flowchart of research was shown in figure 1 and the details of methodology was shown in figure 3.

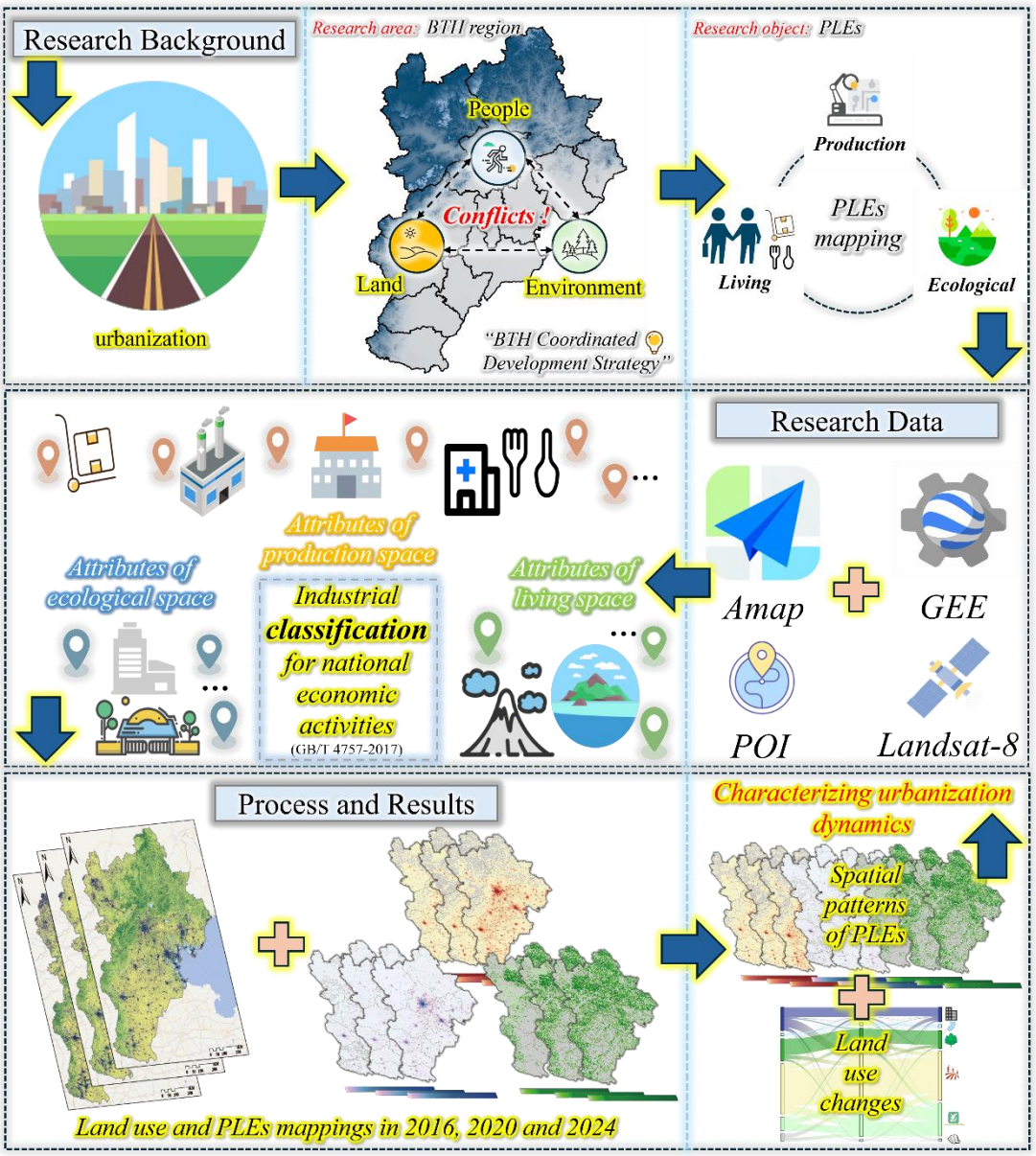

Figure 1: flowchart of research

2. Study area and Materials

2.1 Study Area

The BTH region comprises 13 cities(36°05'N - 42°37'N, 113°11'E - 119°45'E), including Beijing (China's capital) and Tianjin (both direct-controlled municipalities), along with 11 prefecture-level cities in Hebei Province that surround these two major urban centers, covering an area of 216,000 square kilometers (approximately 2.25% of China's total land area) in the Bohai Sea region of Northeast China[58-59]. The terrain features a distinct northwest-to-southeast elevation gradient (Figure 2 (a) and (b)). With a population exceeding 100 million, the BTH region contributed 10.4442 trillion yuan to China's GDP in 2023, accounting for 8.29% of the national total. However, significant development differences remain within the region, particularly between Hebei and the Beijing-Tianjin area. Such as, the urban disposable income gap between Hebei and Beijing has

expended over the years, increasing from 24,400 yuan in 2014 to 38,300 yuan in 2020, and further to 42,700 yuan in 2022[37]. Urbanization rates also exhibit significant regional differences. As shown in Figure 2(c), Beijing has maintained a consistently high urbanization rate above 80%, while Tianjin over the 80% threshold in 2011 (reaching 80.5%) and has since stabilized. They have consistently exceeded the level of national. In contrast, Hebei's urbanization rate, despite steady growth, remains relatively low, only exceeding 60% in 2020 (60.07%) and reaching 62.77% by 2023. We hope that mapping the BTH region's PLEs patterns to characterize urbanization dynamics can provide quantitative evidence for achieving BTH regional integration by 2030 and balancing people-land-environment relationships.

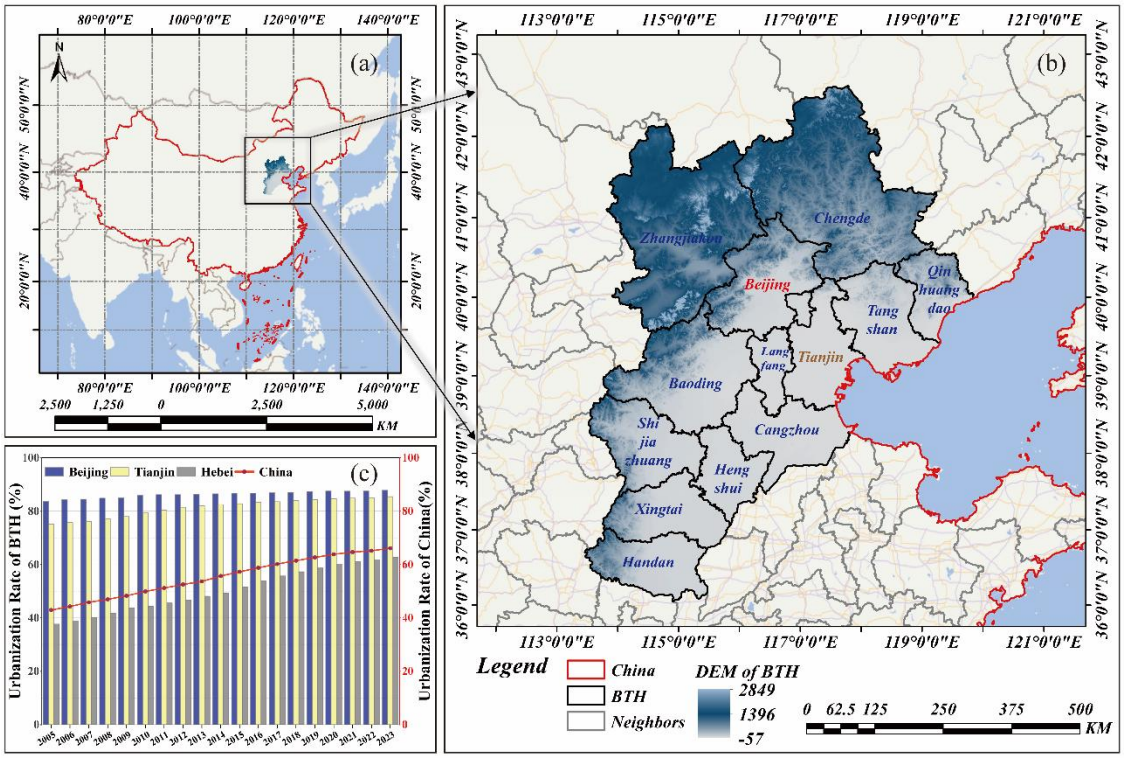

Figure 2. study area

Note: Figure 2(a) shows the geographical location of China in a global context, providing a spatial reference for the study area. Figure 2(b) displays a detailed topographic map of the 13 cities in the BTH region, using Digital Elevation Model (DEM) data to highlight the region's terrain features. All vector-based geographical elements in the figure. were obtained from the National Platform for Common Geospatial Information Services (https://www.tianditu.gov.cn/?4), which uses the WGS-84 coordinate system. The DEM data were sourced from the Google Earth Engine (GEE) platform (https://earthengine.google.com/), a powerful cloud-based geospatial analysis tool. The urbanization rate statistics in Figure 2(c) were collected from the National Bureau of Statistics of China (http://www.stats.gov.cn/).

2.2 Data Resource

This study primarily utilizes two datasets: POI data and Landsat-8 remote sensing imagery. Firstly, as a type of location-based service dataset and social sensing data, POI data has been widely applied in various fields with the advancement of internet and mobile terminal technologies[39]. POI data represents geographical entities of varying sizes and shapes (e.g., shopping malls, mountains, companies) as point features, each containing functional attributes (e.g., company, scenic spot) and

geographic coordinates (latitude and longitude). These attributes are organized into categories, subcategories, and sub-subcategories. For instance, Table 1 illustrates four POI data points (A to D) from the BTH region in 2016. The POI data used in this study spans from 2016 to 2024 and covers the BTH region, sourced from "Amap"[54], one of the three major map service providers in China[52]. Specifically, we collected POI data across 23 categories annually for 13 cities within the region. Secondly, we selected the Dynamic World dataset for our analysis, a remote sensing product that is accessible through Google Earth Engine (GEE). This dataset provides 10-meter resolution near-real-time land use data and covers the entire globe, while it is also compatible with the full Sentinel-2 L1C image archive that has been available since June 27, 2015. Built on Sentinel-2 Top of Atmosphere (TOA) imagery, Dynamic World delivers global land cover updates every 2 to 5 days, with the update frequency differing according to geographic location. Google developed this dataset in partnership with the National Geographic Society and the World Resources Institute for the Dynamic World Project, and it is hosted as an Earth Engine Image Collection under the identifier "GOOGLE/DYNAMICWORLD/V1"[60].

Table 1 Main field attribute of POI data

Name	Location		Field Attribute of Connotation of POI Data		
	longitude	latitude	Category	Subcategory	Sub-subcategory
A	115.47**	39.46**	Scenic Spots	Scenic Spots	Temples and Taoist Sites
B	115.77**	39.27**	Scenic Spots	Scenic Spots	Scenic Spots
C	114.48**	36.60**	Business and Residential	Residential Areas	Residential Communities
D	115.61**	39.61**	Geographical Names	Natural Geographical Names	Mountains

Note: The "***" symbol and the names of points "A, B, C, D" were used for privacy protection, and the geographical coordinates are based on the WGS-84 system. The website of Amap and GEE are (http://www.amap.com) and (https://earthengine.google.com/), respectively.

2.3 Methodology of Research

In the existing literature, the identification and mapping of PLEs have been conducted using various data sources and methods. These include: directly utilizing the attributes of POI data[26], relying only on land use interpretation[23-24], [35], [61-62], combining land use interpretation with POI data[57], integrating land use interpretation with socio-economic data such as population [25], combining POI data with remote sensing data like nighttime light[28], and employing machine learning to integrate land use interpretation, POI data, and multi-source remote sensing data[29]. Regarding the classification of POI data for PLEs, most scholars categorize based on the specific functions of geographic entities, while some refer to relevant national classification standards. For instance, Wang et al. (2024) used the *Urban Land Use Classification and Planning and Construction Land Use Standards* (GB50137-2011)[46], and Ni et al. (2023) applied the Current *Land Use Classification* (GB/T 21010-2017) and the *Code for Classification of Urban and Rural Land Use and Planning Standards of Development Land* (GB 50137-2019)[57].

However, the current classification and mapping processes have several significant limitations. Firstly, the selection of certain indicators is overly subjective, particularly when distinguishing between production and living attributes. Secondly, relying on remote sensing data and land use

interpretation data often neglects the socio-economic attributes of PLEs and the heterogeneity of built landscapes. Additionally, using only POI data, which is recorded by map navigation websites, may result in incomplete coverage of the study area and overlook the natural attributes of ecological functional spaces. Lastly, when multiple data sources are utilized, the process becomes time-consuming and complex, and the essential attributes of PLEs may not be immediately represented due to the excessive and overlapping data attributes.

Above all, in this study, we primarily use POI data, supplemented by land use interpretation, to map PLEs. We classify POI data into PLEs categories based on their attributes, following *China's Industrial classification for national economic activities (GB/T 4757-2017)*, to clearly differentiate between production and living spaces. To address the coverage limitations of POI data at the regional scale, we overlay land use data to integrate socio-economic development with natural ecological processes. Overall, we categorized 23 types of POI data in the BTH region into three space types based on their field attributes. Further details are provided in Table 2.

Table 2: Classification of POI data

Space Type	Field attribute of connotations of POI data
Production Space	Agricultural, forestry, animal husbandry, and fishing bases; industrial parks; factories; power business halls; water supply business halls; corporate enterprises; shopping services; healthcare services; life services; transportation facility and road services; dining and accommodation services; financial and insurance services; motor vehicle services; educational, scientific, and cultural services; government agencies and social organizations, etc.
Living Space	Residential areas, public facilities, scenic spots and historic sites, place names and addresses, etc.
Ecological Space	Natural place names include mountains, rivers, etc.

Additionally, considering the timeline of the BTH coordinated development strategy and the more complete POI data records after 2016, we select three time points—2016, 2020, and 2024—for mapping and comparative analysis. The detailed and overall research methodology are presented in Steps 1-4.

Step 1: Input remote sensing data and POI data

In Step 1, we input remote sensing and POI data. Specifically, Landsat-8 imagery with 30m resolution was processed using Google Earth Engine, while POI data for the BTH region in 2016, 2020, and 2024 were handled in RStudio 4.3.2 and ArcGIS 10.8.

Step 2: Remote sensing interpretation and POI connections

In Step 2, we conducted remote sensing interpretation and POI spatial connections. The land use data were sourced from Dynamic World, which classifies land into nine types: water, forest, grassland, flooded vegetation, farmland, shrub and scrub, built-up land, bare land, and snow and ice. For the BTH region, we applied this classification to the years 2016, 2020, and 2024. The final land use datasets were generated by prioritizing mode values for 10-meter pixels across each full year, with median values used as a supplementary method. Next, we created a 5 km × 5 km grid across the BTH region, clipped by its administrative boundaries, resulting in 150,088 grid cells. Based on the classification system in Table 2, POI points were categorized into three functional attributes: "production space", "living space", and "ecological space". These points were spatially connected to the grid cells using their latitude and longitude coordinates. In the next step, we aim to define and

map each functional space cell based on its connected points.

Step 3: Integrating two types of data for PLEs mapping

For mapping, we adopted the natural breaks method, using a color gradient with five intervals. The shading of each grid cell was based on the percentage (formula (1)) of a specific POI category within the total number of that category in the region. To better visualize and compare the dynamics of the three functional spaces, we generated individual maps for each category rather than integrating them into a single map. However, due to the large scale of the region and limited POI coverage, some grid cells did not have any type of POI data to connect to. These cells, referred to as "NA," numbered 1,528 in 2016, 958 in 2020, and 382 in 2024, representing a small proportion of the total. In Step 3, we supplemented these "NA" cells using land use data. Since POI data is closely tied to socio-economic and urbanization development, areas without POI records are likely to be less developed. Therefore, we used a simplified land use classification to fill these gaps. Specifically, built-up land was assigned to the "living space" attribute, farmland was assigned to the "production space" attribute, and the remaining four land use types (water, forest, grassland, and bare land) were assigned to the "ecological space" attribute. We then calculated the "area proportion" (formula (2)) of each land use type within the "NA" cells relative to the total area of that type across all "NA" cells and used these proportions for data filling. Finally, we integrated these results with the POI-based mapping to complete the global grid-based mapping of the PLEs in the BTH region.

$$Percentage_{ij} = \frac{n_{ij}}{N_i}, (i = P, L, E;\ j = cell_1, ..., cell_m) \tag{1}$$

$$Area\_Persentage_{ij} = \frac{a_{ij}}{A_i}, (i = P, L, E;\ j = cell_1, ..., cell_x) \tag{2}$$

In formulas (1) and (2), i represents the attribute type of POI data or land use, categorized as production (P), living (L), or ecological (E); j represents a specific cell being analyzed; m is the total number of cells that belong to P, L, or E; x denotes the total number of cells that are not connected to any POI data; n denotes the number of POI data points of a specific type within a given cell; N represents the total number of POI data points of that type across all cells; a refers to the land use area of type P, L, or E within a specific cell; and A represents the total land use area of that type across all cells.

Step 4: Urbanization dynamics characterization

In Step 4, we characterized the urbanization dynamics of the BTH region from a functional spatial perspective. This approach enabled a bottom-up analysis, examining both land use changes in 2016, 2020, and 2024, as well as the spatial patterns of the PLEs, while integrating functional zoning with the landscape heterogeneity of built environments. Here, we use the land use transition matrix (formula (3)) to facilitate the extraction of land use changes. By utilizing the land use transition matrix, we can clearly observe the increase and decrease in the six land use types, as well as their specific transitions[23], [63, 64], which helps us further interpret urbanization dynamics.

$$S_{ij} = \begin{bmatrix} S_{11} & S_{12} & \cdots & S_{1m} \\ \cdots & \cdots & \cdots & \cdots \\ \cdots & \cdots & \cdots & \cdots \\ S_{m1} & S_{m2} & \cdots & S_{mm} \end{bmatrix} \tag{3}$$

In formula (3), i represents the initial land use type, m represents the converted land use type, and S represents the specific area.

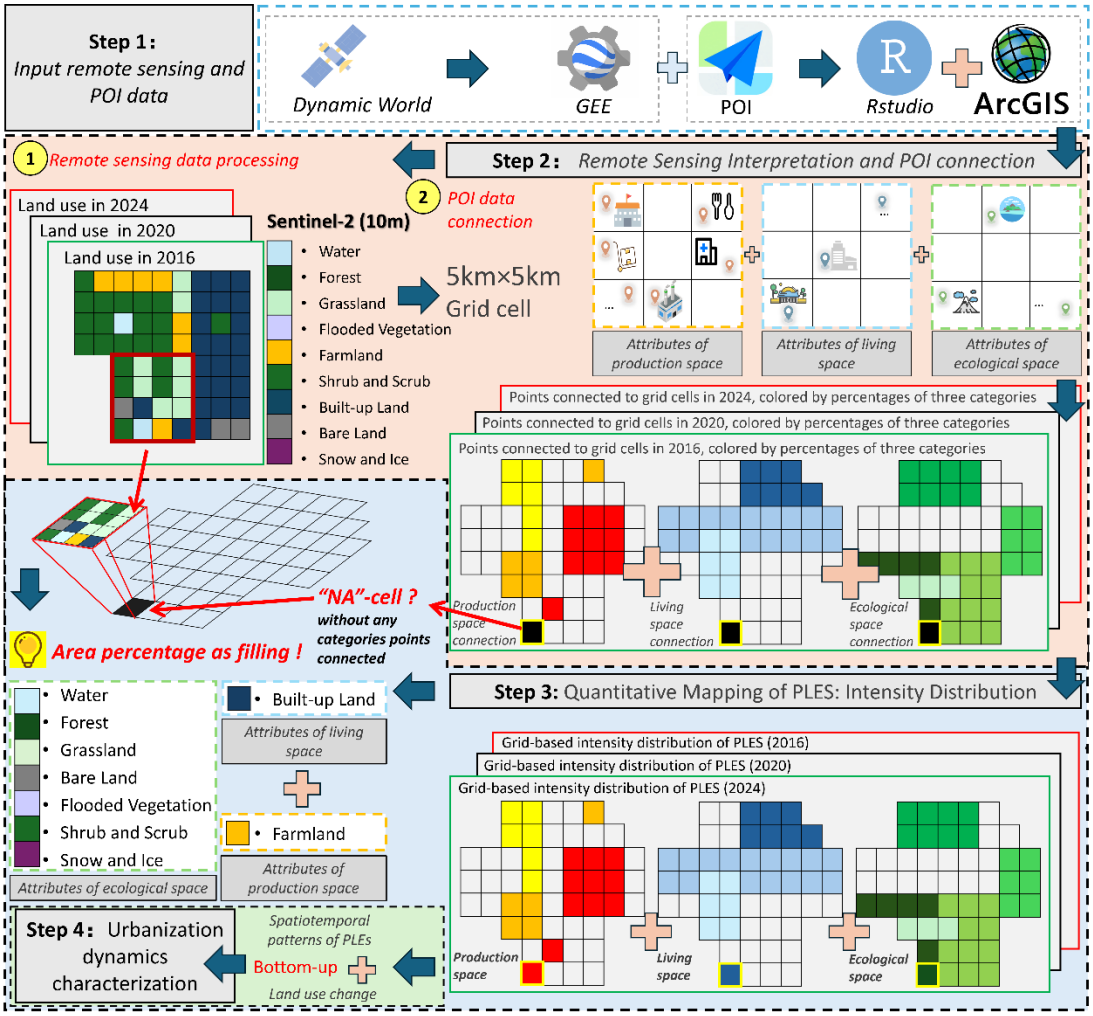

Figure 3: Flowchart of the Methodology in the Research

3. Results

3.1 Land Use Change Characteristics in the BTH Region

During the two study periods, the land use structure in the study area exhibited stage-specific differences: "intense adjustment in the first period and stable restoration in the second period", with significant variations in the magnitude and direction of change across different land use types (Table 3 and Fig.4 (A)).

In terms of area scale, farmland (1.4×10^9, 1.5×10^9 m^2), forest (8.9×10^8, 1.1×10^9 m^2), and built-up land (5.2×10^8, 6.2×10^8 m^2) were the dominant land use types, accounting for over 80% of the total area. In contrast, snow and ice (9.6×10^5, 2.1×10^7 m^2) and flooded vegetation (2.1×10^6, 5.8×10^6 m^2) had the smallest areas, contributing less than 1% of the total.

Regarding system stability, the retention rate of most land use types increased in 2020–2024 compared to 2016–2020. The most significant increase was observed for forest (from 76.11% to 90.59%), followed by water (from 77.82% to 82.45%). Only flooded vegetation showed a slight decrease in retention rate (from 52.19% to 38.18%). These trends indicate a gradual enhancement

in the resilience of the land use system in BTH.

Additionally, from the overall land use data of the Beijing-Tianjin-Hebei (BTH) region and the changes in the built-up areas of Beijing, Tianjin, and Shijiazhuang (the capital city of Hebei Province) presented in Figure 4, the rapid expansion of the built environment and the evolutionary changes in the land use patterns associated with such expansion can be observed in a straightforward and intuitive manner.

Table 3 Core Indicators of Land Use Change in the Study Area (2016–2024)

Type Code	Land Use Type	Net Change Area ($\times 10^6$ m^2)		Net Change Rate (%)		Retention Rate Change (%)
		2016-2020	2020-2024	2016-2020	2020-2024	
0	Water	-0.82	+1.45	-0.77	+1.36	77.82 → 82.45
1	Forest	-190.50	+65.42	-17.53	+7.30	76.11 → 90.59
2	Grassland	-37.62	-10.19	-52.17	-29.54	34.84 → 41.96
3	Flooded Vegetation	+3.72	-0.74	+178.23	-12.82	52.19 → 38.18
4	Farmland	+83.73	-56.75	+5.93	-3.79	91.46 → 89.92
5	Shrub and Scrub	+108.67	-0.32	+32.01	-0.72	71.63 → 73.60
6	Built-up Land	+56.64	+35.95	+10.75	+6.16	92.96 → 93.68
7	Bare Land	-39.84	-12.23	-47.24	-27.49	26.20 → 39.91
8	Snow and Ice	+16.02	-19.68	+346.87	-95.33	15.78 → 1.30

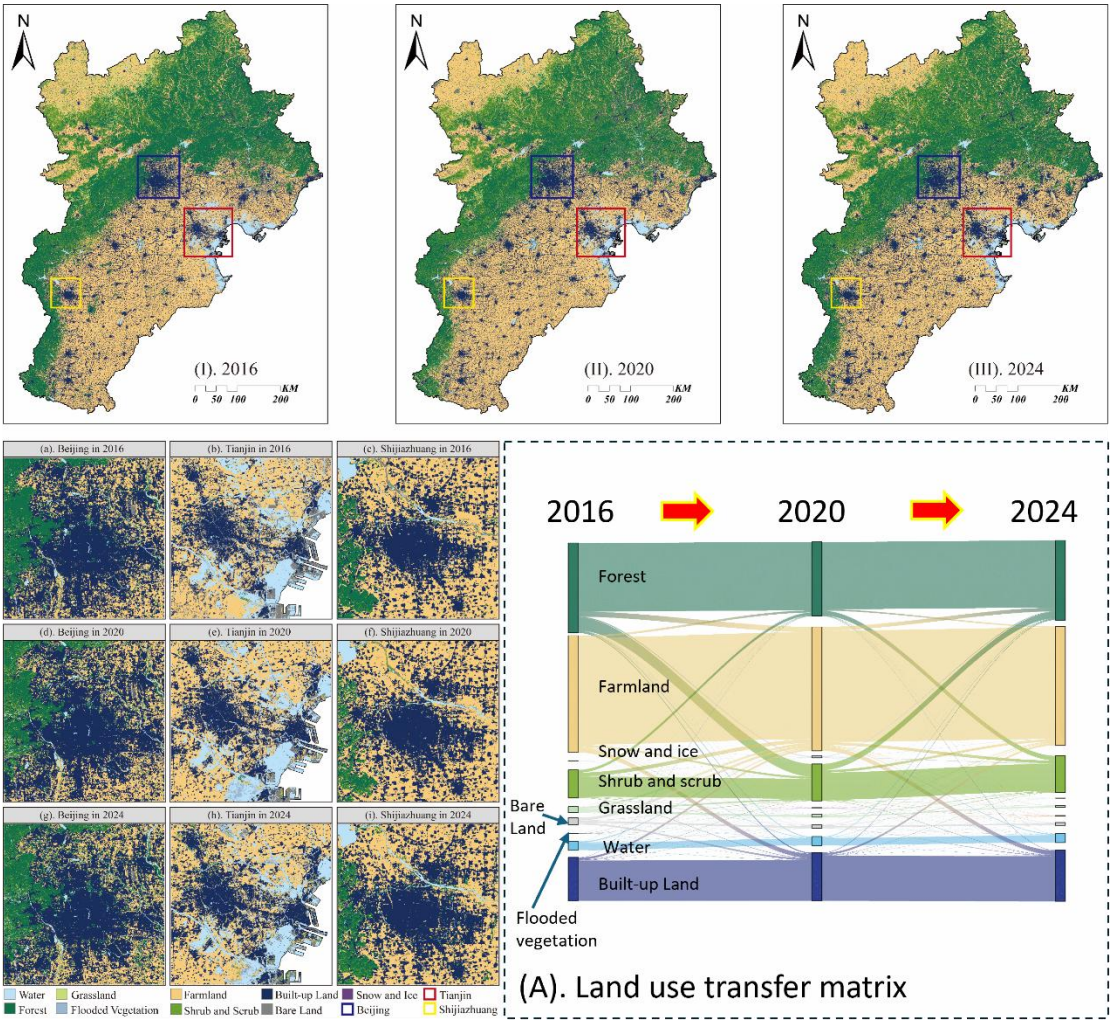

Figure 4: Land use change in the BTH region for the years 2016, 2020, and 2024

3.2 Spatial Patterns of PLEs in the BTH Region

The map uses the natural breaks method to divide the color scale into five levels, with percentages determining the color intensity. Gray grid cells represent non-functional space cell, allowing us to observe the expansion or reduction of specific functional spaces by tracking changes in the number of gray cells out of the total 150,088 space cell. The intensity of color changes also indicates shifts in the strength of these functions. By comparing the mapping results for 2016, 2020, and 2024, the spatiotemporal evolution of the BTH region's PLEs can be summarized as follows:

Specifically, in the BTH region between 2016, 2020, and 2024, living spaces were the dominant type, with the highest number of functional cells and a balanced distribution across the region. The expansion of living spaces was the most noticeable, though most of the newly added cells fell into the lowest intensity category. The number of gray non-living space cells gradually decreased from 1,727 in 2016 to 376 in 2020 and further dropped to 254 by 2024. This expansion was evenly distributed across 11 cities in Hebei Province, with a similar degree of growth. Additionally, high-intensity living space cells were notably concentrated in Beijing, Tianjin, Shijiazhuang, Tangshan, and Baoding. Between 2016 and 2020, there was little change in high-intensity living space cells. However, from 2020 to 2024, these cells began to extend northeast and southwest from Beijing and Tianjin into Hebei Province, forming small clusters and showing a trend of significant increase and fragmentation (Figure 5 (b), (e), and (h)).

For production spaces, the distribution of functional cells across the region was less extensive compared to living spaces but still relatively concentrated. Non-production space cells were mainly found in Zhangjiakou, Chengde, and the border areas of Qinhuangdao and Baoding. The expansion and reduction of production space cells were primarily observed in Zhangjiakou and Baoding. High-intensity production space cells were concentrated in the same areas as living spaces, such as Beijing, Tianjin, Shijiazhuang, Tangshan, and Baoding. From 2020 to 2024, the increase in high-intensity production space cells followed a trend similar to that of living spaces, but their distribution was more fragmented and covered a wider area (Figure 5 (a), (d), and (g)).

Finally, ecological space cells were not only the least distributed but also the most fragmented. The relatively concentrated cells were mainly located in Zhangjiakou and Chengde, with a smaller number in Beijing, Tianjin, and Baoding. The expansion of ecological spaces was most significant between 2016 and 2020, with non-ecological space cells decreasing from 9,510 in 2016 to 8,139 in 2020. From 2016 to 2024, the changes can be summarized as follows: significant expansion of ecological space cells in the Beijing-Tianjin-Zhangjiakou area and its northern regions, with a notable increase in high-intensity cells; meanwhile, areas to the south (especially around Baoding and the western border of Shijiazhuang) showed a trend of increasing in ecological space cells, with fragmentation(Figure 5 (c), (f), and (i)). Additionally, the overlap between ecological space cells and production or living spaces was relatively low.

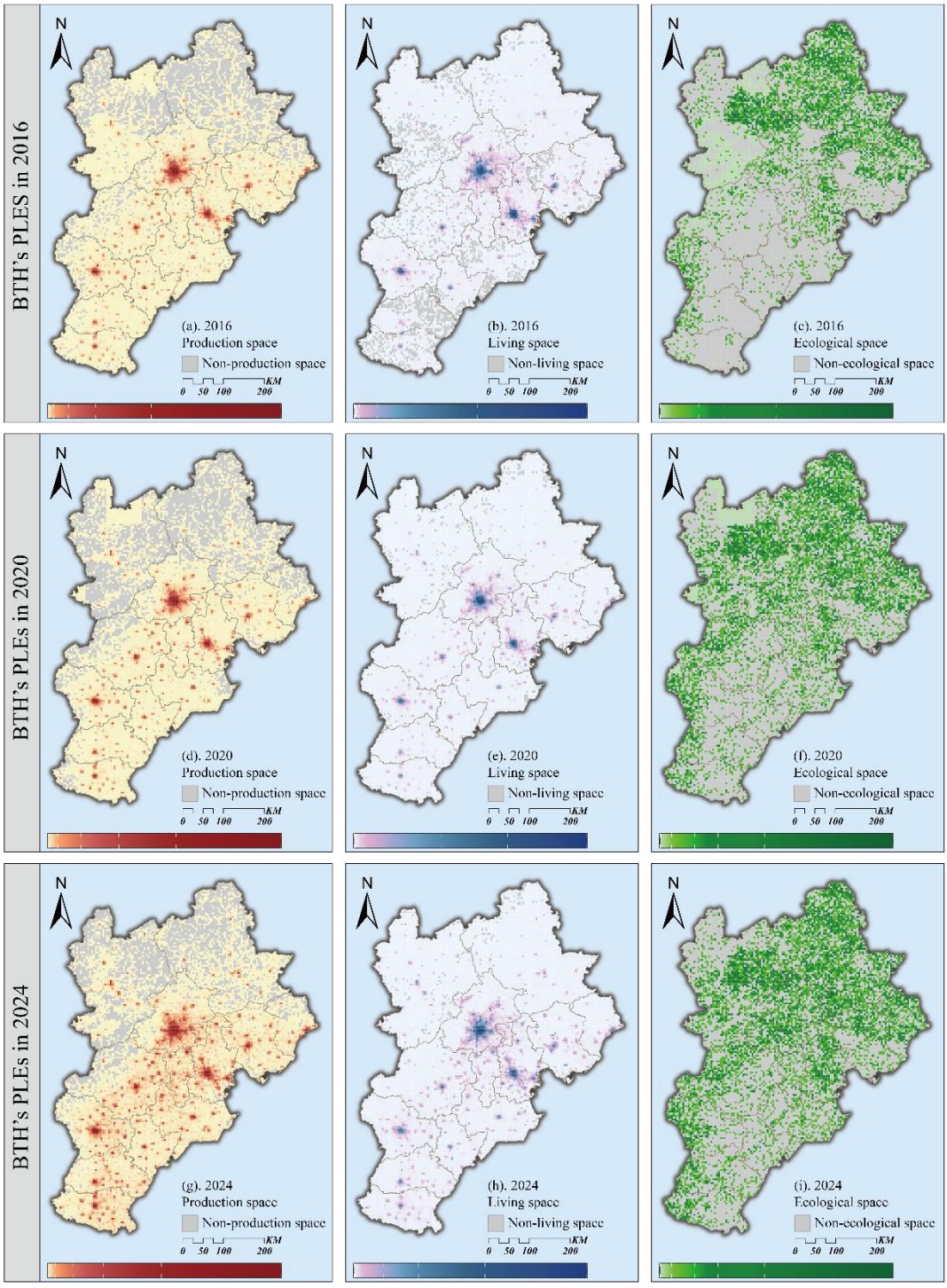

Figure 5: Mapping of PLEs in the BTH region for the years 2016, 2020, and 2024

3.3 Characterizing Urbanization Dynamics: From the Lens of Land Use to PLEs Patterns

By integrating land use change data with the spatiotemporal evolution of grid-based PLEs, this study characterizes the urbanization dynamics of the BTH region from a perspective shifting from land use morphology to functional space attributes, and further reveals the intrinsic coupling

relationship between land use types and PLEs. This dual-perspective analysis enables a more comprehensive understanding of how the human-land-environment system interacts with the urbanization process in the BTH region.

3.3.1 BTH Urbanization Dynamics Foundation from the Lens of Land Use: Two-Stage Evolution

The 2016–2020 period manifested as an intense adjustment stage of land use in the BTH region, shaped by the dual drivers of natural climate fluctuations and early-stage rapid urbanization. This stage was marked by two core characteristics, ecological type polarization and artificial type steady expansion, which directly mapped onto the structural changes of PLE functional spaces. Ecologically, the extreme differentiation of land use types (snow and ice/flooded vegetation growth vs. forest/grassland/bare land loss) translated to the fragmentation and shrinkage of ecological space in the BTH region, with grassland's 52.17% reduction (the highest among all types) and forest's 190.50×10^6 m^2 loss leading to the degradation of ecological buffer zones, while the growth of flooded vegetation (178.23%) partially compensated for wetland ecological space in limited areas. For artificial land use types, the synchronous expansion of built-up land (10.75% growth, 92.96% retention rate) and farmland (5.93% growth) corresponded to the rapid expansion of production and living spaces: built-up land growth directly drove the sprawl of urban living space and industrial production space, while farmland expansion ensured the stability of agricultural production space, reflecting the BTH region's attempt to balance urbanization and food security in the early stage. The reduction of bare land (47.24%) also represented a positive transformation—idle land was converted into production or living space via land consolidation, improving the efficiency of land use for PLE functions.

The 2020–2024 period transitioned to a stable restoration stage, characterized by ecological restoration initiation and artificial expansion deceleration, with the coupling between land use types and PLEs becoming more coordinated under the guidance of ecological policies. The most prominent land use change (forest's 7.30% growth) directly drove the expansion of ecological space in the BTH region's mountainous areas (e.g., Taihang and Yan Mountains), verifying the effectiveness of the "Grain for Green" program in reconstructing ecological functional space; meanwhile, the slowed reduction of grassland (from "- 52.17%" to "- 29.54%") and bare land (from "-47.24%" to "- 27.49%") mitigated the continuous shrinkage of ecological space. Conversely, the near-disappearance of snow and ice (95.33% reduction) due to regional warming led to the loss of alpine ecological space, and the 12.82% reduction of flooded vegetation weakened wetland ecological function, revealing the vulnerability of climate-sensitive land use types in supporting ecological space stability. For artificial-built types, built-up land's shift from "scale-driven" to "quality-oriented" expansion (growth rate down by 4.59 percentage points) meant the optimization rather than sprawl of production and living spaces, the BTH region focused on improving the quality of existing urban functional spaces instead of occupying new land, while farmland's moderate reduction (3.79% decline) reflected a rational adjustment of agricultural production space to accommodate the moderate expansion of urban production and living spaces under the coordinated development strategy.

3.3.2 BTH Urbanization Dynamics from the Functional Space Perspective: reflection for the Interaction Between Humans and Land

Shifting from land use morphology to functional space attributes further unveils the heterogeneous and unbalanced characteristics of BTH's urbanization dynamics, which are

inherently rooted in the spatial differentiation of land use type changes. Production spaces showed a core-periphery fragmentation feature: the sharp increase and fragmentation of high-intensity production cells in southern Hebei (adjacent to Beijing and Tianjin) were directly caused by the spillover of built-up land expansion from core cities to the periphery—industrial land (a subset of built-up land) in Beijing and Tianjin was relocated to southern Hebei, leading to the scattered distribution of production functional cells in the peripheral region. Living spaces exhibited a regional universal expansion feature, with coverage approaching full scale across the BTH region, which stemmed from the widespread improvement of residential land (another subset of built-up land) in both core cities and peripheral areas, reflecting the comprehensive advancement of population urbanization and living facility construction in the region. Ecological spaces presented a northern expansion with fragmentation feature: the significant expansion of ecological spaces in Zhangjiakou and Chengde was mainly driven by forest land restoration and grassland protection in these areas, while the increased fragmentation of ecological functional cells was a result of the patchy distribution of restored forest land and the remaining scattered bare land, highlighting the challenge of connecting ecological space patches despite positive land use restoration.

In terms of spatial overlap, the BTH region's urbanization was characterized by high integration of PLEs and low overlap of ecological spaces, a pattern closely tied to the land use type combination. Production and living spaces overlapped extensively (especially in Beijing and Tianjin) because industrial land and residential land, two key components of built-up land, were highly mixed in core urban areas, forming integrated production-living functional units that remained concentrated and balanced. In contrast, ecological spaces showed low overlap with other functional types and increasing fragmentation, as ecological land use types (forest, grassland, wetland) were intentionally separated from artificial land use types (built-up land, farmland) in the BTH region's land use planning to protect ecological barriers, resulting in the isolated distribution of ecological functional cells. This spatial pattern reflects the inherent trade-off between urban development (based on artificial land use types) and ecological protection (based on natural land use types) in the rapid urbanization of the BTH region.

4 Discussion

4.1 Evaluating BTH Coordinated Development Strategy through PLEs

To build a world-class city agglomeration centered on the capital, the Chinese government implemented the BTH Coordinated Development Strategy. This strategy aims to address current issues such as urban challenges in Beijing and the significant development disparities among Beijing, Tianjin, and Hebei. Over the past decade, up to 2024, the strategy has achieved remarkable progress, as evidenced by statistical data. In this section, we evaluate the policy's effectiveness through a spatial lens by analyzing the spatiotemporal evolution of PLEs maps. Specifically, Figure 5 illustrates that production and living spaces in Hebei Province have continued to expand, accompanied by a significant increase in high-intensity functional space cells in both categories. Meanwhile, Hebei, designated as the target area for ecological functions under the policy, has shown notable improvements in ecological spaces on the PLEs maps. This is particularly evident in regions like Zhangjiakou and Chengde. Overall, the evolution of PLEs aligns closely with the achievements described in the introduction, particularly those related to the policy's primary objective of relocating Beijing's non-capital functions. This demonstrates the effectiveness and utility of the

PLEs spatial analysis in achieving the policy's goals by 2030.

Additionally, given the significant achievements made over the past decade, the experience of the Chinese government in implementing the BTH Coordinated Development Strategy serves as a valuable reference for addressing urbanization challenges. These experiences can be summarized in three key aspects. Firstly, strong policy measures were implemented to remove barriers to the flow of economic, demographic, housing, industrial, and technological factors, preventing their concentration in specific regions and thereby promoting regional integration. Secondly, economic activities, population, and industries were redirected to surrounding areas, fostering resource spillover and shared development through optimal resource allocation. Finally, new built-up areas, such as Xiong'an and the Beijing Sub-Center, were established to accommodate and redistribute functional spaces, supporting sustainable urban development and the integration of the BTH region.

4.2 Advantages of the mapping Methodology

The advantages of the whole methodology can be summarized into three aspects: (1) efficient data integration: Combining POI data with land use data seamlessly integrates socioeconomic activities and natural ecological processes, avoiding complex data layering and excessive statistical processing while directly reflecting PLEs attributes; (2) scientific classification: POI data is categorized into PLEs based on China's national economic industry standards, strengthening the link between socioeconomic and ecological processes and highlighting each space's unique characteristics; (3) Simplicity and applicability: Grid-based functional cell mapping simplifies spatial comparisons and visualization, streamlining the mapping process and enhancing the method's logical consistency and broader applicability.

4.3 Limitations

The main limitation of this study lies in the hierarchical constraints of the mapping process, which prevent further refinement to a more detailed level. Specifically, some attribute fields in the POI data lack clear categorization, making it difficult to accurately distinguish different types of enterprises. For example, under the broad "company and enterprise" category, diverse technology firms are grouped together despite significant functional differences. Additionally, certain fields contain recording inconsistencies, further reducing classification accuracy. As a result, the current PLE mapping framework remains relatively coarse and does not fully capture finer spatial characteristics. To enhance the effectiveness of PLEs as indicators of urbanization, it is crucial to refine classification standards and improve mapping precision. This will allow for a more detailed and dynamic representation of urban functional changes, better aligning with the complexities of rapid urban development.

5. Conclusion

This study addressed the insufficient exploration of the link between urbanization dynamics and PLEs by focusing on the BTH region, a typical area facing integrated development demands. Through innovatively integrating POI and land use data, we developed an optimized grid-level PLE space mapping methodology, one that integrates socioeconomic processes with natural ecological foundations while accounting for urban landscape heterogeneity.

The findings are as follows:

(1) Significant Land Use Changes: From 2016 to 2024, the BTH region underwent a distinct

two-phase evolution in land use rather than following a uniform long-term trend. During the intense adjustment phase (2016-2020), grassland (52.17% reduction), forest (17.53% reduction), and bare land (47.24% reduction) all experienced substantial losses. In contrast, the stable restoration phase (2020-2024) brought a marked reversal: forest cover expanded by 7.30%, while the rate of decline for grassland (29.54% reduction) and bare land (27.49% reduction) slowed significantly. Water bodies remained relatively stable across both phases, with net change rates within ±1.5%. Built-up land continued to grow but at a decelerated pace, with its growth rate falling from 10.75% to 6.16%. Farmland shifted from a 5.93% increase in 2016-2020 to a moderate 3.79% decrease in 2020-2024. These shifts were driven by the dual forces of urbanization transition and the need to balance regional food security in the BTH region.

(2) Evolutions of PLEs Patterns: Among the PLEs, living spaces dominated, featuring the highest number of functional cells and a relatively uniform distribution across the BTH region. By 2024, their coverage neared full scale across the region. Production spaces were spatially concentrated, with high-intensity production cells showing significant overlap with living spaces, particularly in core urban areas such as Beijing and Tianjin. Ecological spaces had the fewest functional cells and remained highly fragmented. They were primarily concentrated in Zhangjiakou and Chengde, the key ecological barrier areas of the BTH region, with only limited distribution in Beijing, Tianjin, and Baoding.

(3) Characterization of Urbanization Dynamics: Urbanization in the BTH region from 2016 to 2024 was centrally characterized by the mutual conversion of built-up land and farmland, alongside the coexistence of ecological restoration and degradation. Spatially, high-intensity production space cells increased sharply and became more fragmented, especially in southern Hebei adjacent to Beijing and Tianjin. This pattern reflects the spillover of industrial functions from core cities to peripheral areas. Ecological spaces expanded notably in Zhangjiakou and Chengde, driven by forest restoration efforts, yet their functional units became increasingly fragmented. Production and living spaces maintained a high degree of overlap, embodying mature mixed urban functions in core cities. While ecological spaces were fragmented, their concentrated distribution in northern BTH formed a complementary ecological protection pattern amid the region's urbanization process.

In summary, our work enriches the understanding of the interplay between urbanization dynamics and urban functional spatial patterns during regional integrated development. It not only provides a novel case study perspective for characterizing urbanization but also offers a new quantitative lens and empirical insights to support the BTH region in achieving its integrated development goals by 2030.

Reference

[1] P. Roberts, "Using urban pasts to speak to urban presents in the Anthropocene," vol. 1, 2024.

[2] T. Elmqvist *et al.*, "Urbanization in and for the Anthropocene," *npj Urban Sustain*, vol. 1, no. 1, p. 6, Feb. 2021, doi: 10.1038/s42949-021-00018-w.

[3] T. Zhou *et al.*, "Addressing the rural in situ urbanization (RISU) in the Beijing–Tianjin–Hebei region: Spatio-temporal pattern and driving mechanism," *Cities*, vol. 75, pp. 59–71, May 2018, doi: 10.1016/j.cities.2018.01.001.

[4] C. Montag, C. Sindermann, D. Lester, and K. L. Davis, "Linking individual differences in

satisfaction with each of Maslow's needs to the Big Five personality traits and Panksepp's primary emotional systems," *Heliyon*, vol. 6, no. 7, p. e04325, July 2020, doi: 10.1016/j.heliyon.2020.e04325.

[5] X. Guan, H. Wei, S. Lu, Q. Dai, and H. Su, "Assessment on the urbanization strategy in China: Achievements, challenges and reflections," *Habitat International*, vol. 71, pp. 97–109, Jan. 2018, doi: 10.1016/j.habitatint.2017.11.009.

[6] E. Wang, J. Song, and T. Xu, "From 'spatial bond' to 'spatial mismatch': An assessment of changing jobs–housing relationship in Beijing," *Habitat International*, vol. 35, no. 2, pp. 398–409, Apr. 2011, doi: 10.1016/j.habitatint.2010.11.008.

[7] S. Zhou, Y. Liu, and M.-P. Kwan, "Spatial mismatch in post-reform urban China: A case study of a relocated state-owned enterprise in Guangzhou," *Habitat International*, vol. 58, pp. 1–11, Nov. 2016, doi: 10.1016/j.habitatint.2016.08.003.

[8] N. S. Wigginton, J. Fahrenkamp-Uppenbrink, B. Wible, and D. Malakoff, "Cities are the Future," *Science*, vol. 352, no. 6288, pp. 904–905, May 2016, doi: 10.1126/science.352.6288.904.

[9] K. C. Seto *et al.*, "From Low- to Net-Zero Carbon Cities: The Next Global Agenda," *Annu. Rev. Environ. Resour.*, vol. 46, no. 1, pp. 377–415, Oct. 2021, doi: 10.1146/annurev-environ-050120-113117.

[10] K. C. Seto, B. Güneralp, and L. R. Hutyra, "Global forecasts of urban expansion to 2030 and direct impacts on biodiversity and carbon pools," *Proc. Natl. Acad. Sci. U.S.A.*, vol. 109, no. 40, pp. 16083–16088, Oct. 2012, doi: 10.1073/pnas.1211658109.

[11] M. T. J. Johnson and J. Munshi-South, "Evolution of life in urban environments," *Science*, vol. 358, no. 6363, p. eaam8327, Nov. 2017, doi: 10.1126/science.aam8327.

[12] B. Güneralp, M. Reba, B. U. Hales, E. A. Wentz, and K. C. Seto, "Trends in urban land expansion, density, and land transitions from 1970 to 2010: a global synthesis," *Environ. Res. Lett.*, vol. 15, no. 4, p. 044015, Apr. 2020, doi: 10.1088/1748-9326/ab6669.

[13] O. Varis, "Curb vast water use in central Asia," *Nature*, vol. 514, no. 7524, pp. 27-29, Oct. 2014.

[14] J. Jiang and T. Zhou, "Agricultural drought over water-scarce Central Asia aggravated by internal climate variability," *Nat. Geosci.*, vol. 16, no. 2, pp. 154–161, Feb. 2023, doi: 10.1038/s41561-022-01111-0.

[15] K. Huang, X. Lee, B. Stone, J. Knievel, M. L. Bell, and K. C. Seto, "Persistent Increases in Nighttime Heat Stress From Urban Expansion Despite Heat Island Mitigation," *JGR Atmospheres*, vol. 126, no. 4, p. e2020JD033831, Feb. 2021, doi: 10.1029/2020JD033831.

[16] K. Huang, X. Li, X. Liu, and K. C. Seto, "Projecting global urban land expansion and heat island intensification through 2050," *Environ. Res. Lett.*, vol. 14, no. 11, p. 114037, Nov. 2019, doi: 10.1088/1748-9326/ab4b71.

[17] F. Meng, "Quantification of the food-water-energy nexus in urban green and blue infrastructure: A synthesis of the literature," 2023.

[18] B. Pandey, C. Brelsford, and K. C. Seto, "Infrastructure inequality is a characteristic of urbanization," *Proc. Natl. Acad. Sci. U.S.A.*, vol. 119, no. 15, p. e2119890119, Apr. 2022, doi: 10.1073/pnas.2119890119.

[19] X. J. Yang, "China's Rapid Urbanization," *Science*, vol. 342, no. 6156, pp. 310–310, Oct. 2013, doi: 10.1126/science.342.6156.310-a.

[20] H. Jiang *et al.*, "An assessment of urbanization sustainability in China between 1990 and 2015 using land use efficiency indicators," *npj Urban Sustain*, vol. 1, no. 1, p. 34, July 2021, doi: 10.1038/s42949-021-00032-y.
[21] X. Kuangdi, "The Progress and Grand Challenge of Urbanization in China," *Engineering*, vol. 2, no. 1, pp. 26–28, Mar. 2016, doi: 10.1016/J.ENG.2016.01.029.
[22] X. Tu, C. Fu, A. Huang, H. Chen, and X. Ding, "DBSCAN Spatial Clustering Analysis of Urban 'Production–Living–Ecological' Space Based on POI Data: A Case Study of Central Urban Wuhan, China," *IJERPH*, vol. 19, no. 9, p. 5153, Apr. 2022, doi: 10.3390/ijerph19095153.
[23] G. Zhou, D. Zhang, Q. Zhou, and T. Shi, "Study on the Spatiotemporal Evolution Characteristics of the 'Production–Living–Ecology' Space in the Yellow River Basin and Its Driving Factors," *Sustainability*, vol. 14, no. 22, p. 15227, Nov. 2022, doi: 10.3390/su142215227.
[24] Y. Zhao, J. Cheng, Y. Zhu, and Y. Zhao, "Spatiotemporal Evolution and Regional Differences in the Production-Living-Ecological Space of the Urban Agglomeration in the Middle Reaches of the Yangtze River," *IJERPH*, vol. 18, no. 23, p. 12497, Nov. 2021, doi: 10.3390/ijerph182312497.
[25] J. Fu, Q. Gao, D. Jiang, X. Li, and G. Lin, "Spatial–temporal distribution of global production–living–ecological space during the period 2000–2020," *Sci Data*, vol. 10, no. 1, p. 589, Sept. 2023, doi: 10.1038/s41597-023-02497-1.
[26] Y. Yang *et al.*, "Spatial Identification and Interactive Analysis of Urban Production—Living—Ecological Spaces Using Point of Interest Data and a Two-Level Scoring Evaluation Model," 2022.
[27] Y. Chen and M. Zhu, "Spatiotemporal Evolution and Driving Mechanism of 'Production-Living-Ecology' Functions in China: A Case of Both Sides of Hu Line," *IJERPH*, vol. 19, no. 6, p. 3488, Mar. 2022, doi: 10.3390/ijerph19063488.
[28] S. Wang, J. Tian, A. Namaiti, J. Lu, and Y. Song, "Spatial pattern optimization of rural production-living-ecological function based on coupling coordination degree in shallow mountainous areas of Quyang County, Hebei Province, China," *Front. Ecol. Evol.*, vol. 11, p. 1169007, May 2023, doi: 10.3389/fevo.2023.1169007.
[29] Z. Bu, J. Fu, D. Jiang, and G. Lin, "Production–Living–Ecological Spatial Function Identification and Pattern Analysis Based on Multi-Source Geographic Data and Machine Learning," *Land*, vol. 12, no. 11, p. 2029, Nov. 2023, doi: 10.3390/land12112029.
[30] J. Zhu, Z. Shang, C. Long, and S. Lu, "Functional Measurements, Pattern Evolution, and Coupling Characteristics of 'Production-Living-Ecological Space' in the Yangtze Delta Region," 2023.
[31] S. Yu, W. Deng, Y. Xu, X. Zhang, and H. Xiang, "Evaluation of the production-living-ecology space function suitability of Pingshan County in the Taihang mountainous area, China," *J. Mt. Sci.*, vol. 17, no. 10, pp. 2562–2576, Oct. 2020, doi: 10.1007/s11629-019-5776-1.
[32] Y. Liu, J. Xu, Y. Zhou, A. Muhtar, and L. Wang, "Spatiotemporal Differentiation of the Coupling and Coordination of Production-Living-Ecology Functions in Hubei Province Based on the Global Entropy Value Method," *IJERPH*, vol. 19, no. 23, p. 16062, Nov. 2022, doi: 10.3390/ijerph192316062.
[33] W. Li, Z. Cai, and L. Jin, "Spatiotemporal characteristics and influencing factors of the

coupling coordinated development of production-living-ecology system in China," *Ecological Indicators*, vol. 145, p. 109738, Dec. 2022, doi: 10.1016/j.ecolind.2022.109738.

[34] Y. Yin and F. Xi, "Simulation of the evolution track of future Production–Living–Ecological Space under the framework of comprehensive assessment of climate change: A case study of Heilongjiang Province, China," *Environmental Technology*, 2023.

[35] H. Li, C. Fang, Y. Xia, Z. Liu, and W. Wang, "Multi-Scenario Simulation of Production-Living-Ecological Space in the Poyang Lake Area Based on Remote Sensing and RF-Markov-FLUS Model," *Remote Sensing*, vol. 14, no. 12, p. 2830, June 2022, doi: 10.3390/rs14122830.

[36] X. Jiang, S. Zhai, H. Liu, J. Chen, Y. Zhu, and Z. Wang, "Multi-scenario simulation of production-living-ecological space and ecological effects based on shared socioeconomic pathways in Zhengzhou, China," *Ecological Indicators*, vol. 137, p. 108750, Apr. 2022, doi: 10.1016/j.ecolind.2022.108750.

[37] Y. Wu and X. Leng, "A Review and Outlook on the 10th Anniversary of the Coordinated Development of the Beijing-Tianjin-Hebei Region," *Economy and Management*, vol. 38, no. 2, pp. 1-8, Mar. 2024.

[38] J. Cheng, "11 Years of Coordinated Development: Beijing-Tianjin-Hebei Embarks on a New Journey," *China Economic Herald*, vol. 001, pp. 1-3, Feb. 22, 2025.

[39] Y. Liang and Y. Hu, "Regional development assessment based on POIs and Geotree: a case study in Beijing-Tianjin-Hebei region," *Environ Dev Sustain*, vol. 26, no. 7, pp. 18785–18809, June 2023, doi: 10.1007/s10668-023-03415-6.

[40] W. Yang, Y. Ye, B. Fan, S. Liu, and J. Xu, "Identifying Land Use Functions in Five New First-Tier Cities Based on Multi-Source Big Data," *Land*, vol. 13, no. 3, p. 271, Feb. 2024, doi: 10.3390/land13030271.

[41] J. Wei, Y. Zhong, and J. Fan, "Estimating the Spatial Heterogeneity and Seasonal Differences of the Contribution of Tourism Industry Activities to Night Light Index by POI," *Sustainability*, vol. 14, no. 2, p. 692, Jan. 2022, doi: 10.3390/su14020692.

[42] Z. Xie *et al.*, "An urban building use identification framework based on integrated remote sensing and social sensing data with spatial constraints," *Geo-spatial Information Science*, pp. 1–25, Aug. 2024, doi: 10.1080/10095020.2024.2387918.

[43] G. Lou, Q. Chen, K. He, Y. Zhou, and Z. Shi, "Using Nighttime Light Data and POI Big Data to Detect the Urban Centers of Hangzhou," *Remote Sensing*, vol. 11, no. 15, p. 1821, Aug. 2019, doi: 10.3390/rs11151821.

[44] P. Lv, X. Li, H. Zhang, X. Liu, and L. Kong, "Research on the Spatial and Temporal Distribution of Logistics Enterprises in Xinjiang and the Influencing Factors Based on POI Data," *Sustainability*, vol. 14, no. 22, p. 14845, Nov. 2022, doi: 10.3390/su142214845.

[45] L. Liu, G. Cheng, J. Yang, and Y. Cheng, "Population spatialization in Zhengzhou city based on multi-source data and random forest model," *Front. Earth Sci.*, vol. 11, p. 1092664, Aug. 2023, doi: 10.3389/feart.2023.1092664.

[46] Y. Wang and S. Yang, "Identification of surface thermal environment differentiation and driving factors in urban functional zones based on multisource data: a case study of Lanzhou, China," *Front. Environ. Sci.*, vol. 12, p. 1466542, Sep. 2024, doi: 10.3389/fenvs.2024.1466542.

[47] Y. Zhou, X. He, and Y. Zhu, "Identification and Evaluation of the Polycentric Urban Structure: An Empirical Analysis Based on Multi-Source Big Data Fusion," *Remote Sensing*, vol. 14, no.

11, p. 2705, June 2022, doi: 10.3390/rs14112705.
[48] J. Yan, P. Feng, F. Jia, F. Su, J. Wang, and N. Wang, “Identification of secondary functional areas and functional structure analysis based on multisource geographic data,” *Geocarto International*, vol. 38, no. 1, p. 2191995, Dec. 2023, doi: 10.1080/10106049.2023.2191995.
[49] L. Jiang, B. Wang, C. Wen, T. Zhang, and J. Zhou, “Exploring the Spatial Pattern of Retail Businesses in Chengdu Based on the Coupling of Nighttime Light Image and POI Data,” *Sustainability*, vol. 17, no. 2, p. 780, Jan. 2025, doi: 10.3390/su17020780.
[50] L. Zhou, Y. Shi, and J. Zheng, “Business Circle Identification and Spatiotemporal Characteristics in the Main Urban Area of Yiwu City Based on POI and Night-Time Light Data,” *Remote Sensing*, vol. 13, no. 24, p. 5153, Dec. 2021, doi: 10.3390/rs13245153.
[51] Y. Zhang, J. Liu, Y. Wang, Y. Cao, and Y. Bai, “Research on the Method of Urban Jobs-Housing Space Recognition Combining Trajectory and POI Data,” *IJGI*, vol. 10, no. 2, p. 71, Feb. 2021, doi: 10.3390/ijgi10020071.
[52] Z. Jun, Y. Xiao-Die, and L. Han, “The Extraction of Urban Built-Up Areas by Integrating Night-Time Light and POI Data—A Case Study of Kunming, China,” *IEEE Access*, vol. 9, pp. 22417–22429, 2021, doi: 10.1109/ACCESS.2021.3054169.
[53] C. Lu *et al.*, “Mapping Urban Spatial Structure Based on POI (Point of Interest) Data: A Case Study of the Central City of Lanzhou, China,” *IJGI*, vol. 9, no. 2, p. 92, Feb. 2020, doi: 10.3390/ijgi9020092.
[54] Y. Fang, H. Yu, Y. Chen, and X. Fu, “Spatial Distribution Characteristics and Influencing Factors of the Retail Industry in Ningbo City in Eastern China Based on POI Data,” *Sustainability*, vol. 16, no. 17, p. 7525, Aug. 2024, doi: 10.3390/su16177525.
[55] B. Xue, X. Xiao, and J. Li, “Identification method and empirical study of urban industrial spatial relationship based on POI big data: a case of Shenyang City, China,” *Geography and Sustainability*, vol. 1, no. 2, pp. 152–162, June 2020, doi: 10.1016/j.geosus.2020.06.003.
[56] D. Yang, P. Xu, and X. Yang, “Exploring the Spatio-Temporal Evolutionary Characteristics of Paomo Restaurants in Xi’an’s Central Urban Area through POI Data Analysis,” *Applied Sciences*, vol. 14, no. 11, p. 4715, May 2024, doi: 10.3390/app14114715.
[57] M. Ni, Y. Zhao, C. Ma, W. Jiang, Y. Xie, and X. Hou, “Spatial Identification and Change Analysis of Production-Living-Ecological Space Using Multi-Source Geospatial Data: A Case Study in Jiaodong Peninsula, China,” 2023.
[58] Y. Wang, H. Liu, G. Mao, J. Zuo, and J. Ma, “Inter-regional and sectoral linkage analysis of air pollution in Beijing–Tianjin–Hebei (Jing-Jin-Ji) urban agglomeration of China,” *Journal of Cleaner Production*, vol. 165, pp. 1436–1444, Nov. 2017, doi: 10.1016/j.jclepro.2017.07.210.
[59] X. Ren, R. Xiong, and T. Ni, “Spatial network characteristics of carbon balance in urban agglomerations– a case study in Beijing-Tianjin-Hebei city agglomeration,” *Applied Geography*, vol. 169, p. 103343, Aug. 2024, doi: 10.1016/j.apgeog.2024.103343.
[60] C. F. Brown *et al.*, “Dynamic World, Near real-time global 10 m land use land cover mapping,” *Sci Data*, vol. 9, no. 1, p. 251, June 2022, doi: 10.1038/s41597-022-01307-4.
[61] Y. Chen, X. Su, and X. Wang, “Spatial Transformation Characteristics and Conflict Measurement of Production-Living-Ecology: Evidence from Urban Agglomeration of China,” *IJERPH*, vol. 19, no. 3, p. 1458, Jan. 2022, doi: 10.3390/ijerph19031458.
[62] T. Zhang *et al.*, “Research on Sustainable Land Use in Alpine Meadow Region Based on

Coupled Coordination Degree Model—From Production–Living–Ecology Perspective," *Sustainability*, vol. 16, no. 12, p. 5213, June 2024, doi: 10.3390/su16125213.

[63] Y. Zhou, X. Li, and Y. Liu, "Land use change and driving factors in rural China during the period 1995-2015," *Land Use Policy*, vol. 99, p. 105048, Dec. 2020, doi: 10.1016/j.landusepol.2020.105048.

[64] W. Liu, J. Zhan, F. Zhao, H. Yan, F. Zhang, and X. Wei, "Impacts of urbanization-induced land-use changes on ecosystem services: A case study of the Pearl River Delta Metropolitan Region, China," *Ecological Indicators*, vol. 98, pp. 228–238, Mar. 2019, doi: 10.1016/j.ecolind.2018.10.054.